Use of digital image correlation to determine the mechanical behavior of materials

*F.M. Sánchez-Arévalo, G. Pulos**

Instituto de Investigaciones en Materiales, Universidad Nacional Autónoma de México, Cd. Universitaria A. P. 70-360, 04510, Mexico

ARTICLE DATA

Article history:
Received 10 December 2007
Received in revised form
31 January 2008
Accepted 1 February 2008

Keywords:
Digital image correlation
Shape memory alloy
CuAlBe
Bovine pericardium
Mechanical behavior

ABSTRACT

Digital image correlation was used to study the mechanical behavior of three materials: commercial aluminum, bovine pericardium and Cu–Al 11.2 wt.%–Be 0.6 wt.% shape memory alloy. These materials were subjected to simple tension test using an MTS load frame with an attached optical microscope. Displacement, force, strain data and digital images of the sample's surface were acquired. Data and images were post-processed in order to measure displacement vector fields for each material. Local and global strain measurements were calculated hence the young modulus was obtained for each material. The elastic moduli were 60 GPa for aluminum, 160 MPa for bovine pericardium and 110 GPa for the CuAlBe austenitic phase and 27 GPa for the mixture of austenite and martensitic phases.

1. Introduction

New experimental techniques have appeared and they have shown more precise results about the mechanical behavior of materials. Particularly, digital image correlation (DIC) has been used to estimate the optical flow on sequences of images using different methods [1–6]. In addition, with DIC has been possible to observe the local mechanical behavior of materials like metals, ceramics and polymers [7–9]. From the local behavior, strain measurements have been calculated in order to determine the elastic properties of materials like steel, polycrystalline silicon, brittle materials and polymers; it has been done using DIC [7,9–11]. The vast majority of these works have used artificial optical texture to improve the development of DIC algorithms at reduced scales as reported in literature [12,13]. Although many works have been done to determine the mechanical behavior of materials using DIC nobody has explored the microstructural or fiber interactions of materials under simple tension using their natural or semi-natural optical texture. The objective of this research was to determine the micro and macro mechanical behavior of three materials with different natural optical textures and with different mechanical responses under simple tension.

In this work the Willert and Gharib algorithm has been employed to detect the optical flow on the sequences of images [6]. The strain measurements are important because they allow an estimate of the elastic parameters of materials to be made. There are several sensors to measure strain; nevertheless, not all sensors are capable of getting a good measure. That is why the sensor of strain has to be selected depending on the material. In this work two metallic materials and a soft biological material are studied. Hence the selected strain sensors were the following: On metallic materials a

* *Corresponding author*. Tel.: +5255 5622 4503; fax: +5255 5622 4602.
E-mail address: gpulos@servidor.unam.mx (G. Pulos).

1044-5803/$ – see front matter © 2008 Elsevier Inc. All rights reserved.
doi:10.1016/j.matchar.2008.02.002

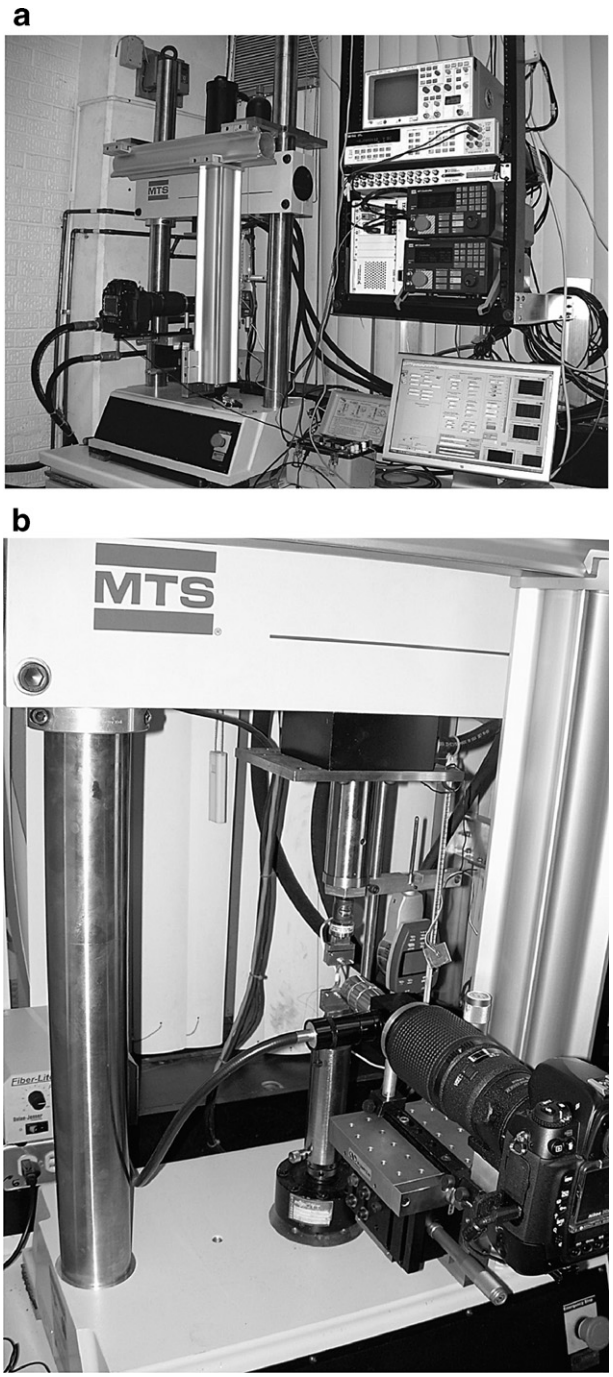

Fig. 1 – Experimental set up.

strain gage, a linear variable differential transformer (LVDT) – which is a sensor that measures the overall displacement of the load frame – and DIC were used, and for the soft material a

Table 1 – Dimensions of specimens

Material	Equivalent length (mm)	Width (mm)	Thickness (mm)
Aluminum	25.88	3	0.99
Bovine pericardium	29.52	5	1.29
CuAlBe	25.88	3	0.68

Table 2 – Surface preparation

Material	Optical texture	Method	Substance
Aluminum	natural	–	–
Bovine pericardium	Semi-natural	Dyed	Methylene blue $C_{16}H_{18}ClN_3S{\cdot}3H_2O$
CuAlBe	Semi-natural	Chemical etching	Ferric chloride $FeCl_3$

LVDT and DIC were used. The measures of strain with the LVDT and the strain gage are considered as macro-mechanical measurement. The measurements that were done with DIC

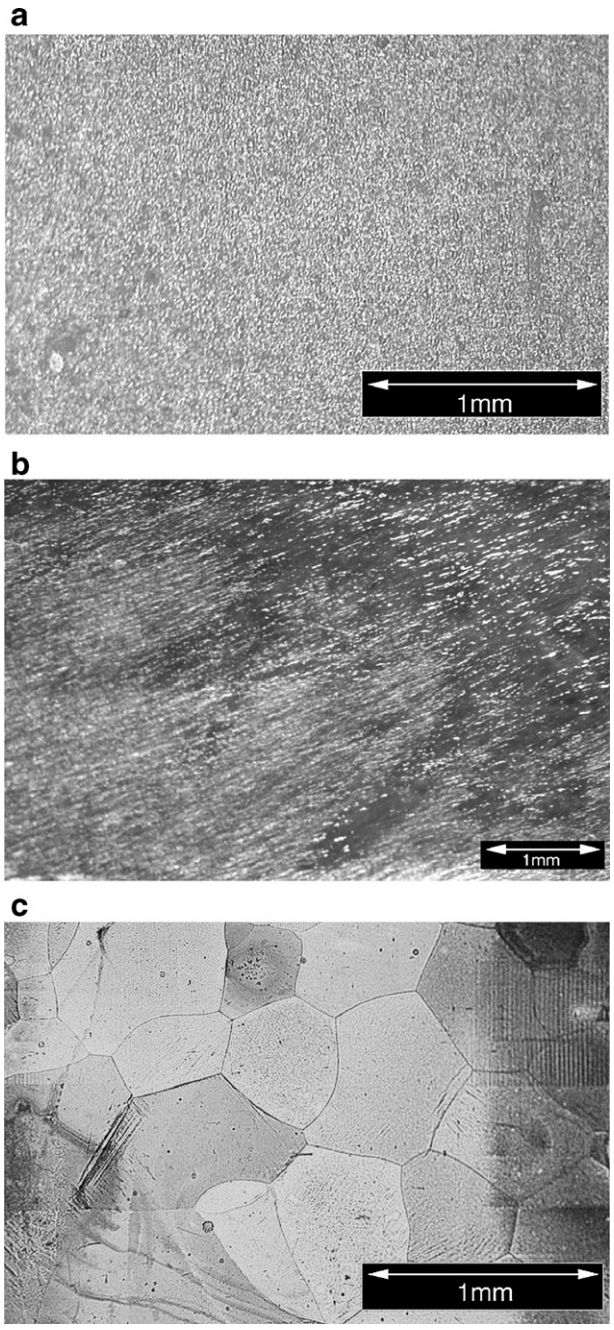

Fig. 2 – Optical textures of materials.

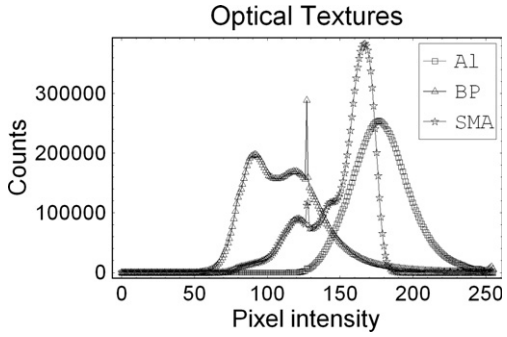

Fig. 3 – Pixel intensity distribution of each texture.

and their strain criteria are considered as micromechanical measurements [14].

2. Experimental Procedure

Tensile tests were performed on a servohydraulic loading device (MTS 858 MiniBionix axial). For digital image correlation an optical microscope was adapted to a high resolution digital camera – Nikon D2X 12Mpix – as shown in Fig. 1. The modular microscope works as an infinity-corrected compound microscope with magnifications of 10X (metallic samples) or 5X (bovine pericardium).

To control the MiniBionix MTS a 407 MTS controller was used while data and image acquisition was supported by National Instruments PXI-1002 and PXI-boards (6281, 8331 and 4220) and a PC. A virtual instrument was programmed in LabVIEW in order to synchronize and save the data and images. The virtual instrument was able to save the following parameters: time, displacement, force, strain and digital images. With the displacement, strain and force data, the macroscopic stress–strain curve was obtained and also images were associated to them. Hence the micro and macro-mechanical behavior of aluminum, bovine pericardium and CuAlBe were observed.

2.1. *Sample Preparation*

The metallic materials were machined in a CNC machine and dogbone tensile specimens were obtained. A special jig was used to cut the bovine pericardium tensile specimen. All dimensions are shown in Table 1.

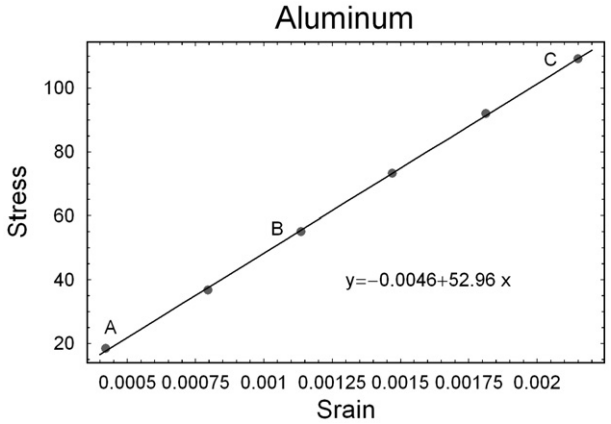

Fig. 4 – Aluminum stress–strain curve.

2.2. *Surface Preparation*

The three different optical textures were obtained by different methods. They are summarized in Table 2.

3. Results

The optical textures of the three materials are shown in Fig. 2. Fig. 2(a) shows that the aluminum specimen presents a natural randomly speckle pattern. The bovine pericardium

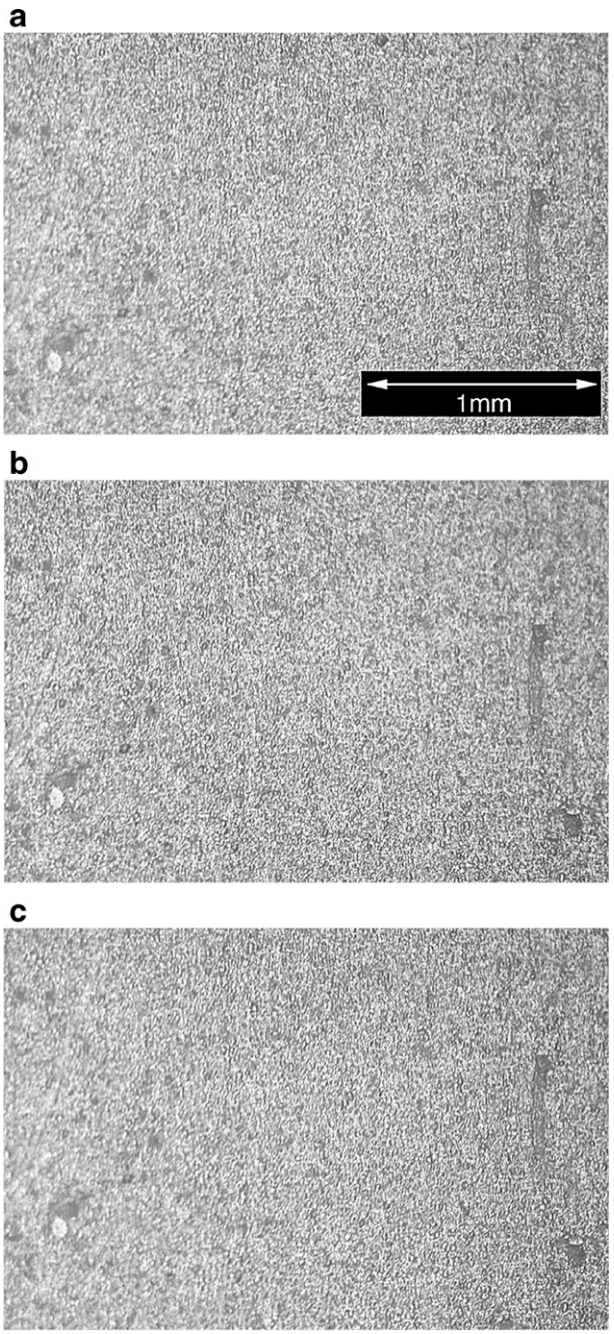

Fig. 5 – Acquired images of the aluminum surface.

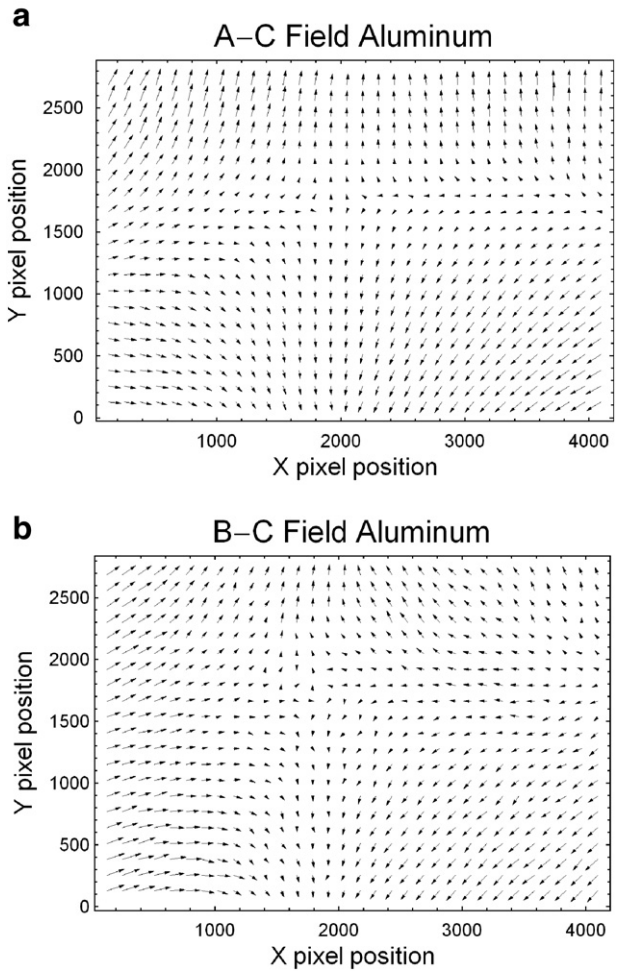

Fig. 6 – Displacement fields of Al, without rigid body motion.

and CuAlBe do not present the same speckle pattern. The optical texture of the CuAlBe alloy shown in Fig. 2(c) reveals the different grains in the alloy. The optical textures possess a bell-shape distribution. This bell-shape distribution is appropriate to image correlation as was reported in the literature [12]. The pixel intensity distribution is shown for each material in Fig. 3. The aluminum shows the best pixel intensity distribution to image correlation.

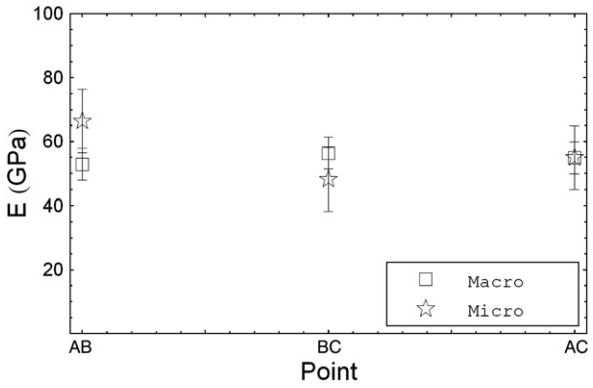

Fig. 7 – Micro and Macro elastic modulus of aluminum.

3.1. *Aluminum*

With the prepared surface of each tensile specimen, a simple tension test was done. In Fig. 4 the stress–strain curve for aluminum is shown. This curve presents the linear mechanical behavior of Al. Hence a linear model was used to fit the experimental data.

Fig. 4 shows three letters A, B and C with increments in strain of about 0.08% (between A and B) and 0.2% (between C and D). These letters are associated to the acquired images, which are shown in Fig. 5.

Using DIC and the acquired images of the aluminum, the displacement vector fields, without rigid body motion, were obtained. These fields are presented in Fig. 6; it shows two hyperbolic fields with elongation in the vertical direction and contraction in the horizontal direction. The first field is due to the applied strain while the second one covers almost the second half of the applied strain. In both cases the fields show no distortion, which corresponds to a homogeneous strain field.

From the displacement fields and the acquired data it was possible to determine the elastic modulus of this material. As shown in Fig. 7, the micro and macro modulus was around 60GPa.

3.2. *Bovine Pericardium*

The bovine pericardium stress vs elongation ratio curve shows a non-linear mechanical behavior. This material also presents a greater range of strain than aluminum; that is why elongation ratio is used instead of strain. This curve has four letters (A, B, C and D, Fig. 8), which were associated to the acquired images during the tensile test. Hence the analysis of the mechanical behavior was concentrated from A to D. A parabolic model was used to represent the elastic modulus from A to D and the macro elastic modulus was determined.

As it was previously mentioned the speckle pattern of the images of bovine pericardium is not the best one; nevertheless, it allow using DIC satisfactorily due to the dying and illumination conditions.

From the above images (Fig. 9) the displacements vector fields were determined, Fig. 10. These fields represent an ideal hyperbolic field and also show a homogeneous mechanical behavior. Hence the elastic modulus was calculated at the micro and macro level too, as shows in Fig. 11.

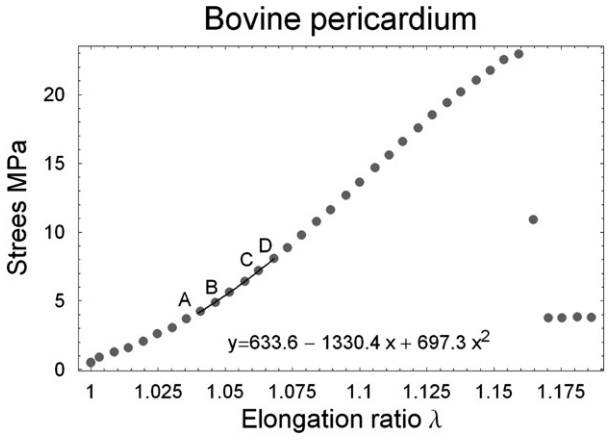

Fig. 8 – Stress–strain curve of bovine pericardium.

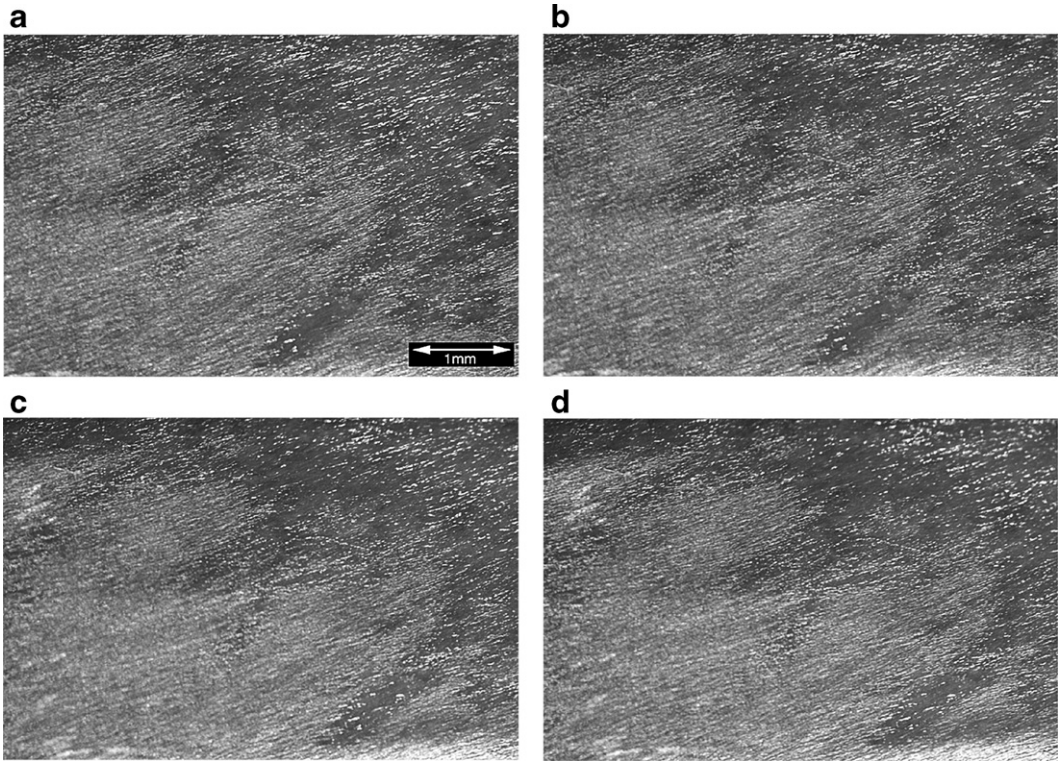

Fig. 9 – Acquired images of the surface of bovine pericardium.

The micro and macro elastic modulus of bovine pericardium is presented in Fig. 11; both measurements are in a good agreement with an elastic modulus around 140 MPa. A decrement in elastic modulus was observed in the CD point which may be due to some fibers fail at that force level.

3.3. *CuAlBe*

The stress vs elongation ratio curve for the CuAlBe shape memory alloy is presented in Fig. 12. It shows the typical mechanical behavior, reported in literature, for this kind of material. The mechanical response of this material is also non-linear but it can be separated in two linear parts, Fig. 12. Hence a linear model was fit to each part. The first one corresponds to the austenite mechanical behavior and the second one corresponds to a mixture of the austenite plus martensite phases.

In the above figure four letters are shown and they correspond to the images in Fig. 13. In this case the material was polished and chemically etched so DIC works with a different optical texture. This semi-natural texture allows observing the grain behavior and the rise of the martensite plates.

The analysis from image C and image D in Fig. 13 pertain to the austenite phase and the displacement vector field is showed in Fig. 14(a). In this figure also a hyperbolic field is observed but it is not completely homogeneous due to the inherent anisotropy in the austenitic phase ([1]). The displacement vector field in Fig. 14(b) shows a higher non-homogeneity due to inherent anisotropy and the anisotropy induced by the mixture of austenite and martensite phases.

The elastic modulus for CuAlBe was calculated for several points including CD and GH. This result shows the evolution of elastic modulus due to the appearance of the stress-induced martensite phase. The modulus for austenite (CD point) is 110 GPa while the modulus for the mixture of phases is around 27 GPa at the GH point (Fig. 15).

4. Conclusions

Digital image correlation can be used to measure displacement fields in natural and semi-natural texture of different materials due to their optical texture which has a quasi-Gaussian distribution in pixel intensity. The displacement vector field for aluminum and bovine pericardium were homogenous; however, it is non homogeneous for CuAlBe. DIC is able to measure the local contributions of the martensite plates although thus martensite plates can also produce illumination changes and errors in DIC. DIC can be used with increments in strain that range from 0.02% in Al through 2.7% in pericardium; thus, DIC seems an appropriate tool to be used in phase transformation studies of shape memory alloys where the strains increments are in the order of 0.25% for a CuAlBe alloy. Aluminum was used as reference material and the calculated elastic modulus with DIC and electrical extensometry for aluminum is in good agreement. The elastic moduli were 60 GPa for aluminum, 160 MPa for bovine pericardium and 110 GPa for the CuAlBe austenitic

[1] The austenitic phase has the anisotropy typical of cubic systems since its elastic constants are: C11=148.2GPa, C12=125.4 GPa and C44=93.5 GPa [15]. Using Zener's anisotropy index [16] A=2 C44/(C11–C12)=10.7 gives a ratio that is quite different from that of an isotropic material [1].

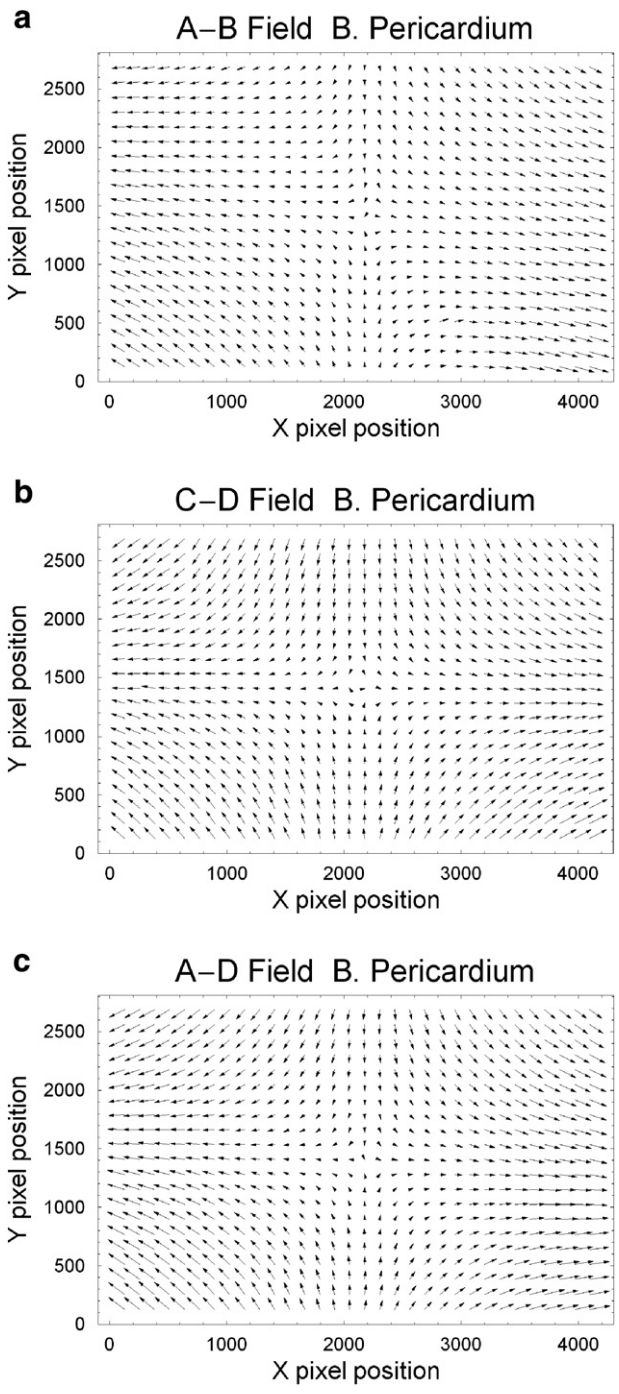

Fig. 10 – Displacement fields of bovine pericardium, without rigid body motion.

phase and 27 GPa for the mixture of austenite and martensitic phases.

Acknowledgments

This work was developed with financial support from the PAPIIT DGAPA-UNAM program through grants IN110601, IN1106005 and IX121504 and CONACyT through grants NC-204 and Salud-2002-C01-8175. The authors are grateful to Gabriel A. Lara for making the CuAlBe Alloy, Manuel Farfan for providing pericardium samples and Mario Acosta for the use of the electrical strain gage equipment.

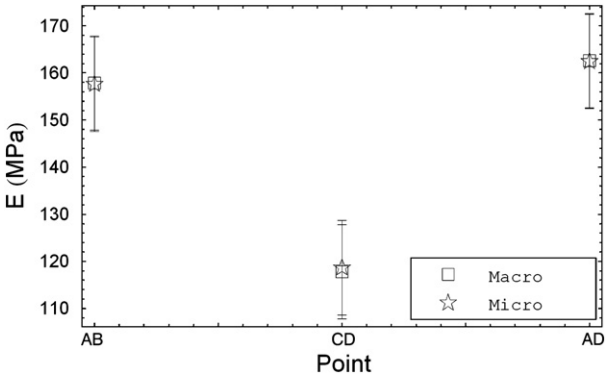

Fig. 11 – Micro and macro elastic modulus of bovine pericardium.

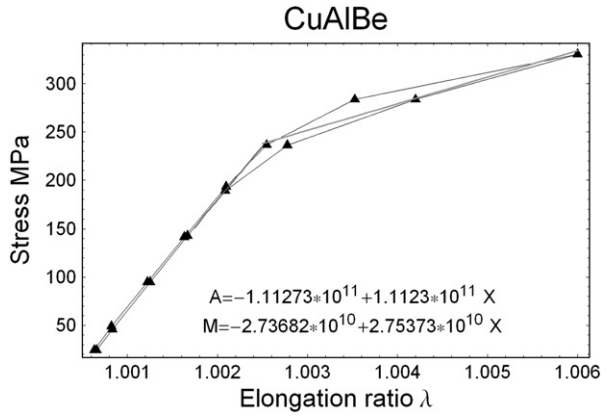

Fig. 12 – Stress–elongation ratio curve of CuAlBe (load and unload).

REFERENCES

[1] Fenneman C, Thompson W. Velocity determination in scenes containing several moving objects. Comput Graph image process 1979;9:301–15.
[2] Nagel HH. Displacement vectors derived from second-order intensity variations in image sequences. Comput Graph image process 1983;21:85–117.
[3] Nagel HH. On the estimation of optical flow: relations between different approaches and some new results. Artif Intell 1987;33:299–324.
[4] Barron JL, Flett DJ, Beauchemin SS, Burkitt TA. Performance of opticalflow techniques. IEEE 1992;0-81862855-3/92:236–42.
[5] Hild F. Correli: A software for displacement field measuremets by digital image correlation. Universidad de Paris; 2002. Internal report no. 254.
[6] Willert CE, Gharib M. Digital particle image velocimetry. Exp fluids 1991;10:181–93.
[7] Sutton MA, Cheng M, Peters WH, Chao YJ, McNeill SR. Application of optimized digital correlation method to planar deformation analysis. Image vis comput 1986;4:143–50.

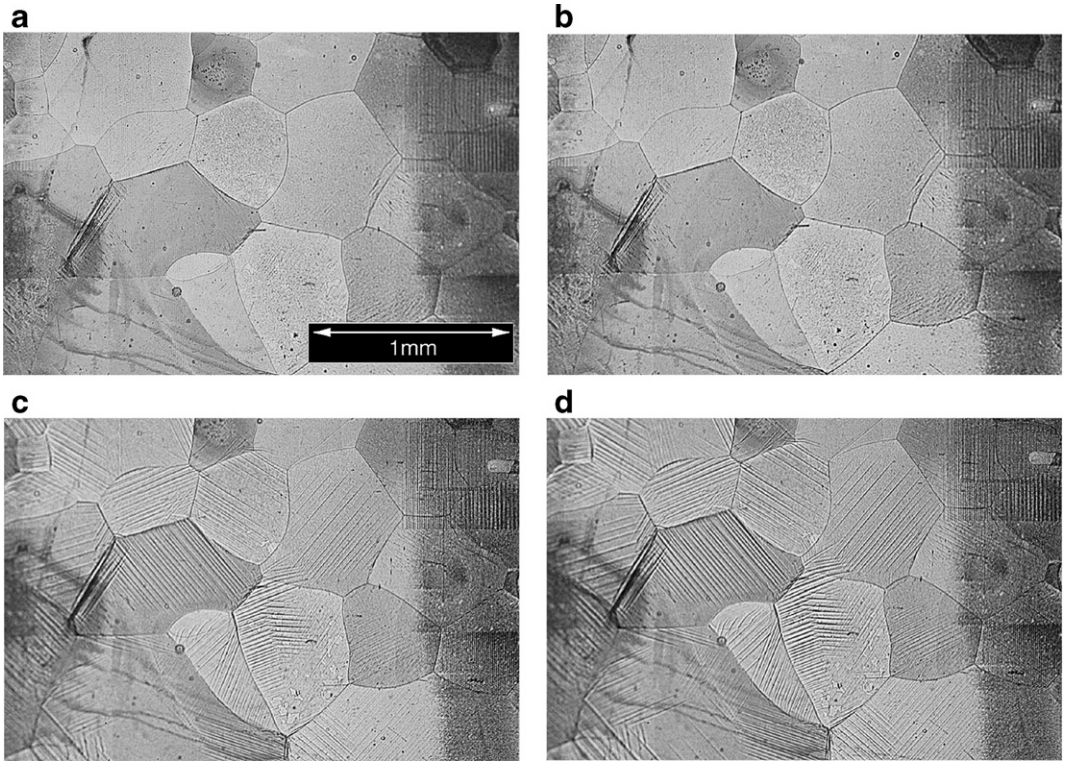

Fig. 13 – Acquired images of the surface of CuAlBe.

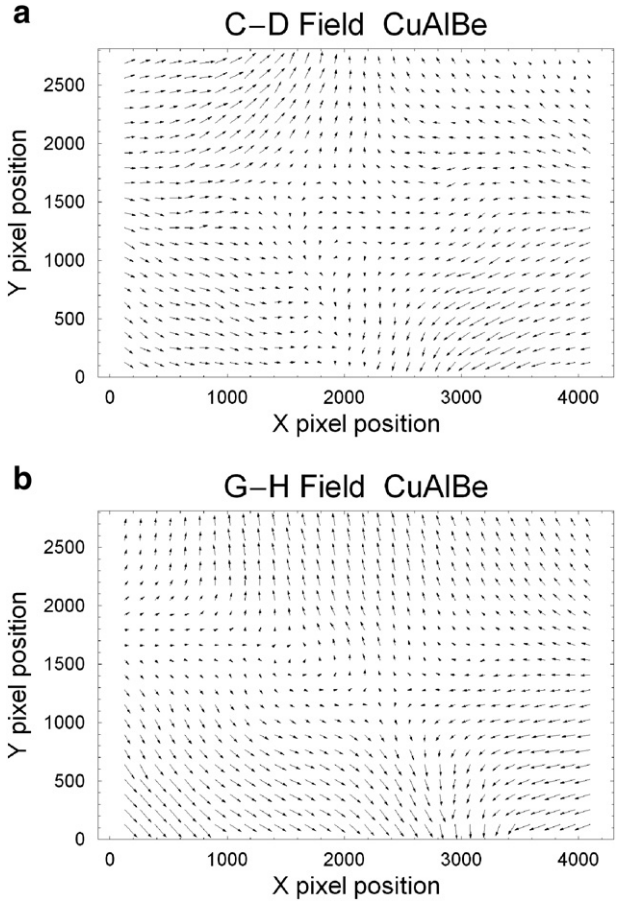

Fig. 14 – Displacement fields of CuAlBe, without rigid body motion.

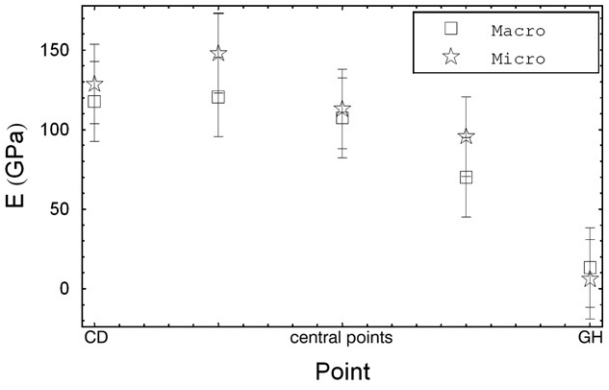

Fig. 15 – Evolution of the elastic modulus.

[8] Chevalier L, Calloch S, Hild F, Marco Y. Digital image correlation used to analyze the multiaxial behavior of rubber-like materials. Eur J Mech A Solids 2001;20:169–87.
[9] Watrisse B, Chrysochoos A, Muracciole JM, Némoz Guillard M. Analysis of strain localization during tensile test by digital image correlation. Eur J Mech A Solids 2000;20:189–211.
[10] Chasiotis I, Knauss W. A new microtensile tester for the study of MEMS materials with the aid of atomic force microscopy. Exp mech 2002;42(1):51–7.
[11] Hild F, Peire JN, Lamon J, Puyo-Pain M. On the use of image digital correlation to analyze the mechanical properties of matrix composites. Advances in Ceramic Matrix Composites XI; 2002. p. 63–76.
[12] Berfield TA, Patel JK, Shimmin RG, Braun PV, Lambros J, Sottos NR. Micro-and nanoscale deformation measurement of surface and internal planes via digital image correlation. Exp Mech 2007;47:51–62.

[13] Scrivens WA, Luo Y, Sutton MA, Collete SA, Myrick ML, Miney P, Colavita PE, Reynolds AP, Li X. Development of patterns for digital image correlation measurements at reduced length scales. Exp Mech 2007;47:63–77.
[14] Sánchez F. M., 2007. Estudio experimental del comportamiento mecánico de un material con memoria de forma. Doctoral Thesis, Universidad Nacional Autónoma de México. Mexico, D. F. pp. 116.
[15] Rios D, Belkahla S, Canales A, Flores H, Guenin G. Elastic constants measurements of Cu–Al–Be alloys. Scr metall mater 1991;25:1351–5.
[16] Zener C. Elasticity and Anelasticity of Metals. Chicago: University of Chicago Press; 1948. p. 16.